SECURITY INFORMATION

[redacted]

Copy 210
RM L52F06

[redacted]

NACA RM L52F06

TECH LIBRARY KAFB, NM
0144356

NACA

RESEARCH MEMORANDUM

7343

LONGITUDINAL STABILITY AND CONTROL CHARACTERISTICS OF A CANARD MISSILE CONFIGURATION FOR MACH NUMBERS FROM 1.1 TO 1.93 AS DETERMINED FROM FREE-FLIGHT AND WIND-TUNNEL INVESTIGATIONS

By Howard J. Curfman, Jr., and Carl E. Grigsby

Langley Aeronautical Laboratory
Langley Field, Va.

CLASSIFIED DOCUMENT

[redacted]

...ized person is prohibited by law.

NATIONAL ADVISORY COMMITTEE
FOR AERONAUTICS
WASHINGTON
August 8, 1952

SECURITY SIGNATURE
REQUIRED

[redacted]

[redacted]

Classification cancelled (or changed to Unclassified)

By (Authority Nasa Tech Pub Announcement #102
(OFFICER AUTHORIZED TO CHANGE)

By ..... 22 June 56

NK
GRADE OF OFFICER MAKING CHANGE)

5 Apr. 61
DATE

TECH LIBRARY KAFB, NM
0144356

NATIONAL ADVISORY COMMITTEE FOR AERONAUTICS

RESEARCH MEMORANDUM

LONGITUDINAL STABILITY AND CONTROL CHARACTERISTICS OF A CANARD MISSILE CONFIGURATION FOR MACH NUMBERS FROM 1.1 TO 1.93 AS DETERMINED FROM FREE-FLIGHT AND WIND-TUNNEL INVESTIGATIONS

By Howard J. Curfman, Jr., and Carl E. Grigsby

SUMMARY

The supersonic longitudinal stability and control characteristics of a canard missile configuration as determined from flight tests of rocket-powered models and supersonic wind-tunnel tests have been compared. The flight tests covered a Mach number range from 1.1 to about 1.6 representing a Reynolds number range of about 10×10^6 to 20×10^6, based on wing mean aerodynamic chord. The wind-tunnel tests were at Mach numbers 1.62 and 1.93 with Reynolds numbers of 0.65×10^6 and 0.58×10^6, respectively.

The results from the two techniques showed good correlation for the slopes of the lift and moment coefficients against angle of attack and for aerodynamic-center location. The nonlinearities in these stability derivatives were present to the highest Mach number attained. The control effectiveness of the deflected canard fins was shown to be practically a pure moment with very little change in lift, the over-all lift effectiveness of the configuration being due to the ability of the canard fins to change the angle of attack. The average moment effectiveness as indicated by the flight tests was higher than that shown by the wind-tunnel results. The use of the stability derivatives as determined by both techniques in predicting the longitudinal frequency-response characteristics gave satisfactory agreement.

INTRODUCTION

The aerodynamic characteristics of missile configurations have received intensified study in recent years. This paper compares

[redacted]

characteristics of a canard missile configuration as determined by free-flight tests using rocket-powered models and supersonic wind-tunnel results. The wind-tunnel data are presented herein, and the flight results are as presented in references 1 and 2. This configuration has been used as a research vehicle in the transonic and supersonic speed regions, and, in addition to obtaining aerodynamic information, evaluations of automatic stabilization systems have also been conducted. References 1, 2, and 3 give information on the longitudinal and roll characteristics of the configuration and include the control effectiveness of canard elevators and wing-tip ailerons. In the material presented herein, only those longitudinal data from both techniques which can be compared directly are given.

SYMBOLS

C_L	lift coefficient, Lift/qS
C_m	pitching-moment coefficient, Moment/$qS\bar{c}$
C_D	drag coefficient, Drag/qS
q	dynamic pressure, lb/sq ft
S	total wing area in one plane, formed by extending leading and trailing edges to center line, sq ft
V	velocity, ft/sec
$\bar{c}$	wing mean aerodynamic chord, ft
α	angle of attack, deg
δ	canard-fin deflection
M	Mach number

$$C_{L_\alpha} = \frac{\partial C_L}{\partial \alpha}$$

$$C_{m_\alpha} = \frac{\partial C_m}{\partial \alpha}$$

$$C_{L_\delta} = \frac{\partial C_L}{\partial \delta}$$

$$C_{m_\delta} = \frac{\partial C_m}{\partial \delta}$$

[redacted]

S_f exposed canard-fin area in one plane, sq ft

I_y moment of inertia in pitch, slug-ft^2

m mass, slugs

$$C_{m_q} = \frac{\partial C_m}{\partial \frac{\dot{\theta}\bar{c}}{2V}}$$

$$C_{m_{\dot{\alpha}}} = \frac{\partial C_m}{\partial \frac{\dot{\alpha}\bar{c}}{2V}}$$

$\dot{\theta}$ pitching velocity, radians/sec

$\dot{\alpha}$ time rate of change of angle of attack, radians/sec

ω forcing frequency, radians/sec

$\left|\dot{\theta}/\delta\right|$ amplitude ratio, radians per sec/radian

DESCRIPTION OF MODELS

The flight model of reference 1, designated model A herein, had cruciform wings and all-movable canard control surfaces of approximately 60° delta plan form. The aerodynamic arrangement was such that the horizontal wings and controls were in the same plane. These surfaces were mounted on a cylindrical body of fineness ratio 16.3 having ogival nose and tail sections of about 3.5 calibers. The wings and canard surfaces had modified double-wedge airfoil sections with constant thicknesses corresponding to a thickness ratio of about 3 percent at the wing-body juncture and about 3 percent at the canard root chord.

The flight model of reference 2, designated herein as model B, was like model A in many general aspects but was not geometrically similar. Model B was approximately 0.875 scale of model A. The wind-tunnel model, model C, was more nearly geometrically similar to model A, differing slightly in the length of the cylindrical portion of the fuselage. The tunnel model was approximately 0.0875 scale of model A. To illustrate more clearly the differences between the three models, figure 1 and table 1 are prepared; in these presentations the ratio of diameters is the linear scale factor used to convert dimensions of models B and C to correspond to those of model A. The boattailing of models A and B was

impractical in the wind tunnel, and in figure 1 the dotted lines indicate the relative sting-windshield position and size. Figure 2 shows the details of the exposed wing and canard surfaces with dimensions corresponding to model A.

TEST TECHNIQUES

Rocket-Powered Model Tests

In the rocket-powered model tests of references 1 and 2, the model contained no sustainer or internal rocket motor but was boosted to the maximum supersonic velocities by means of solid-propellant rocket motors. During the coasting flight from supersonic to subsonic Mach numbers following booster separation, data were continuously transmitted by telemeter and recorded at ground stations. In general, these data included longitudinal and normal accelerations, angle of attack, and total and static pressures. In addition, radar tracking data and radiosonde information were available.

The longitudinal stability and control derivatives were obtained by analyzing the model response to programmed step inputs of the canard longitudinal control surfaces. The period and damping characteristics of the transients and the measurements of steady state or trim values allowed a determination of the stability and control derivatives from the use of the general equations of motion considering two degrees of freedom longitudinally for each available transient. A detailed discussion of this technique is presented in the appendix of reference 2.

For model A the programmed control-surface deflections were of a square wave with deflections of 2.68° and -4.42°. The reason for this approach was that such a method would generally give trim values of angle of attack of slightly different magnitudes and could thus indicate the presence, if any, of nonlinear regions in the various parameters. For model B the square-wave input involved control deflections of $\pm 5^{\circ}$.

Wind-Tunnel Tests

All the wind-tunnel test results presented herein were obtained in the Langley 9-inch supersonic tunnel which is a continuous-operation closed-circuit type in which the stream pressure, temperature, and humidity conditions can be controlled. Different test Mach numbers are provided by interchanging nozzle blocks which form test sections approximately 9 inches square. Throughout the wind-tunnel tests, the moisture content in the tunnel was kept sufficiently low so that the

effects of condensation in the supersonic nozzle were negligible. Eleven fine-mesh turbulence-damping screens are provided in the relatively large area settling chamber just ahead of the supersonic nozzle.

The wind-tunnel model was sting-supported and the sting and sting-windshield arrangement used in these test is illustrated in figure 3. At each angle of attack, the model, sting, and sting windshield were translated across the tunnel so that a fixed point on the model (center-of-gravity location of $0.586\bar{c}$ ahead of leading edge of $\bar{c}$) could be kept on the center line of the tunnel. By use of this arrangement, configurations, which at an angle of attack of 0° were free from shock reflections, could be tested through the angle range of $\pm 15^{\circ}$. Throughout the tests the gap between the rear of the movable windshield was less than 0.012 inch. The sting and sting-windshield arrangement, illustrated in figure 3, has been shown by other tests to have negligible effect on the aerodynamic characteristics of the model.

Measurements of lift, drag, and pitching moment were made by means of external self-balancing mechanical scales through an angle-of-attack range of -5° to 15° for canard-fin deflection angles of 0°, 3°, 6°, 10°, and 15°. Measurements of the pressure in the sting-windshield and balance enclosing box, which tests have shown to be equal to the model base pressure, were made and the drag results were corrected to the condition of base pressure equal to stream pressure. An optical system employing a small mirror mounted in the rear of the model was used to measure angles of attack.

Test Conditions

The Reynolds number of the flight tests of model A (ref. 1), based on the wing mean aerodynamic chord, varied from 10×10^6 to 20×10^6 for the Mach numbers from 1.1 to 1.63, respectively. For model B (ref. 2) the Reynolds number variation was from 10×10^6 to 15×10^6 for Mach numbers from 1.1 to 1.45, respectively. The Reynolds numbers of the wind-tunnel tests at Mach numbers of 1.62 and 1.93 were 0.65×10^6 and 0.58×10^6, respectively.

Accuracy

The accuracy which may be expected from the free-flight tests of rocket-powered models is affected by many considerations, including telemetering and recording errors, velocity errors resulting from both radar and pressure measurements, reading errors, and others.

Reference 2 contains a discussion on accuracy and gives the following as the estimated probable errors in the stability derivatives and coefficients of interest in the present paper for $M = 1.40$:

Percent of given value for -				
C_{L_α}	C_{m_α}	C_{L_δ}	C_{m_δ}	C_D
2	4	40	6	4

While no discussion of the accuracy of the flight tests results of reference 1 is detailed therein, the accuracy is believed to be reasonably the same as that given for the flight tests of reference 2, since the technique of data reduction and instrumentation was essentially the same.

The precision of the wind-tunnel results has been evaluated by estimating the uncertainties in the balance measurements involved in a given quantity and combining these errors by a method based on the theory of least squares.

A summary table of precision estimates follows:

Lift coefficient, C_L	±0.0002
Drag coefficient, C_D	±0.0003
Pitching-moment coefficient, C_m	±0.001
Angle of attack, α, deg	±0.01
Canard-fin deflection angle, δ, deg	±0.25

RESULTS AND DISCUSSION

The flight results presented herein were taken directly from references 1 and 2. The wind-tunnel results at Mach numbers 1.62 and 1.93 are presented in figure 4 with the pitching-moment coefficient referenced to a center-of-gravity location of $0.568\bar{c}$ ahead of the leading edge of the mean aerodynamic chord. The various characteristics of the curves of figure 4 are discussed in detail in the sections which follow.

Lift

The variation of the lift-curve slope C_{L_α} with Mach number is shown in figure 5. The wind-tunnel points are given for $\delta = 3^\circ$ in the small angle-of-attack region $(0 < \alpha < 2^\circ)$ and for $\delta = 6^\circ$ in the angle-of-attack region greater than 2° to correspond more closely to flight

results. The correlation of flight and wind-tunnel results for C_{L_α} is considered quite good. The wind-tunnel data confirm the nonlinearity in lift-curve slope indicated by the flight test of reference 1 and reveal a slope change of about the same magnitude. The tunnel results indicate that this nonlinearity persists at the highest Mach number tested. The wind-tunnel curves of figure 4 show that the nonlinear lift-coefficient curve could in general be represented by two linear segments with the break at about $\alpha = 2^\circ$. Similar nonlinear characteristics have been observed on other canard configurations (see, for example, ref. 4). The reduction in lift-curve slope with Mach number was nearly identical with that calculated for a thin triangular wing from linearized theory.

Static Stability

The variation of aerodynamic-center location with Mach number as determined from the flight and tunnel tests is shown in figure 6. The wind-tunnel points are given for $\delta = 0^\circ$, 3°, and 6° and were taken at trim from the slopes of the $C_m - C_L$ curves. It is noted that where the trim α is near zero, the aerodynamic-center location is somewhat forward from the positions indicated for the trim values of α for the larger control deflection; this is due to the downwash effects being greater at angles of attack very near zero. Since the downwash effects are dependent on the angle of attack, it is expected, of course, that the indicated aerodynamic-center location as determined from plots for the two center-of-gravity locations might vary at trim conditions for the same control deflection. In general, however, these differences amount to a maximum of about $0.03\bar{c}$ for $\delta = 3^\circ$ and 6° at trim for the two flight-test locations of the centers of gravity. Though the canard deflections of model B were $\pm 5^\circ$, the forward center-of-gravity location resulted in smaller trim angles of attack than for model A, and the results indicate a more forward aerodynamic-center location. The data from model B, however, indicate a slightly greater forward shift than can be noted in the tunnel results. With this exception, just noted, the flight and wind-tunnel tests show good agreement. The forward movement of the aerodynamic center with Mach number was also found to be slightly more rapid than that indicated theoretically for the body-triangular-wing combination (no canard surfaces) discussed in reference 5.

The static pitching-moment derivative C_{m_α} is considered here in addition to the discussion of aerodynamic-center location, since the frequency of the short-period mode of motion of the configuration is almost entirely dependent on this parameter. The variation of this derivative with Mach number is presented in figure 7. The wind-tunnel data presented here were determined for the corresponding center-of-gravity locations with respect to the mean aerodynamic chord as existed in the

flight tests. In the comparisons shown, the wind-tunnel data were used for $\delta = 0^{\circ}$, 3°, and 6° with the slopes at trim presented, and the agreement is quite reasonable.

The nonlinearity in $C_{m_{\alpha}}$ indicated by the flight tests of model A and by the tunnel tests is also noted for the canard configurations of reference 4 and is clearly shown from the wind-tunnel results in figure 4. This characteristic is more pronounced in the regions of small angle of attack. The nonlinearity of C_m against α has been noted on many canard configurations with inline surfaces and is the well-known result of the downwash field at the rear wings. The reduction in stability noted in the tunnel tests at angles of attack greater than 10° is probably due to separation effects. The effects of similar changes in $C_{m_{\alpha}}$ on the problem of applying automatic control equipment to this configuration have been studied in reference 6, and the considerations therein lead to the conclusion that the magnitude of the slope changes in the region of small angles of attack as shown herein should cause no great problem in the automatic stabilization and control of this aircraft.

Control Effectiveness

The flight tests of references 1 and 2 showed that the horizontal canard surfaces produced very small changes in total lift but were effective in producing a pitching moment to change the angle of attack. These results are confirmed by the wind-tunnel tests. The very low values of $C_{L_{\delta}}$ are believed to be due to the effect of the downwash from the deflected canard surfaces on the wings, the change in lift on the wings due to downwash being opposite and nearly identical to the lift on the canard fins. Although $C_{L_{\delta}}$ was the least accurate of the parameters presented in reference 2, there was reported therein negative values of this derivative in the supersonic range to $M = 1.44$. The effect of the downwash from the deflected canard fins onto the wings also results in an increase in the pitching moment since the wings and canards are on opposite sides of the center of gravity. Hence, the effectiveness of the deflected canard fins can be described as producing practically a pure moment or couple while of itself causing very little change in lift, the over-all lift effectiveness of the configuration being due to the ability of the canards to change the angle of attack.

The wind-tunnel results of C_L against δ at constant α are presented in figure 8 for both test Mach numbers. The slopes of these curves are noted to be quite small; this plot indicates, however, that the slope trend is positive, the largest value being about 0.001. Values of $C_{L_{\delta}}$ from -0.0026 at $M = 1.1$ to -0.0013 at $M = 1.44$ are shown in

reference 2. Because of the accuracy involved in determining this parameter by both techniques, perhaps the lift effectiveness of the canards can be summarized as being negligible in magnitude but with indications that the slope C_{L_δ} may be positive or negative for the configuration with the present canard-wing locations and relative areas and spans of canards to wings. References 7, 8, and 9 are results of supersonic wind-tunnel tests of other canard configurations; these references show small values of C_{L_δ}, in each case less than 0.003. It might well be mentioned that the wind-tunnel tests referred to in the preceding discussion were all conducted at a Reynolds number of less than 1×10^6. Since the flight tests of reference 2 were in the Reynolds number range of from 10×10^6 to 15×10^6, and if the accuracy involved does not affect the slope trend, the possibility exists that the negative values of C_{L_δ} reported therein (and also indicated in other unpublished flight-test data) are a result of scale effects, but are still very small in magnitude in the low supersonic range considered here.

The wind-tunnel results of C_m against δ at constant α are presented in figure 9 and are cross plots from faired curves. These curves indicate changes in the slope C_{m_δ} with canard deflection, angle of attack, and Mach number. In general, there seems to be a slight reduction in C_{m_δ} at the large canard deflections and at the higher angles of attack for all canard deflections. The curves also are fairly smooth for $M = 1.62$ but tend to be more nonlinear at the higher angles of attack at $M = 1.93$.

The curves of figure 9 also show the reduction in the control effectiveness parameter C_{m_δ} as the Mach number is increased. Figure 10 presents C_{m_δ} against Mach number. The data for models A and B are also shown as presented in references 1 and 2, respectively. The wind-tunnel results are shown for both center-of-gravity locations at angles of attack of 2° and 4° and are faired values of C_{m_δ} for the lower deflection range. While the tunnel results tend, in general, to appear somewhat low compared to the flight results, the over-all picture of the reduction in C_{m_δ} with Mach number is apparent. It is emphasized that the flight results were obtained from changes in trim conditions and the measured values of the static stability derivative C_{m_α}; hence, for the noted nonlinear variations of C_m with α, this method of linear analysis can only afford a mean or average value of C_{m_δ}. Thus, if it is only assumed that the flight data are indicative of the mean or average control effectiveness, figure 10 shows that the reduction in control effectiveness with Mach number noted from the flight tests up to $M = 1.6$ is continued to the higher Mach number, 1.93.

[redacted]

In figure 11 the wind-tunnel results of α_{trim} against δ are presented for the two center-of-gravity locations. These curves indicate that the rate of change of trim α with canard deflection becomes appreciably reduced as the control deflection is increased. No flight results are presented for comparison because of the flight methods of obtaining comparable data. In the flight tests α_{trim} against Mach number was found for the two values of control deflection and the ratio $\frac{\Delta\alpha_{trim}}{\Delta\delta}$ was formed as a function of Mach number. The known presence of nonlinearities in C_m against α and model out-of-trim precludes the use of this ratio as being directly comparable to the slope measured in figure 11. It is apparent, therefore, that the flight technique cannot show the true shape of the α_{trim} against δ curve.

Application of Results

Since the combination of the aircraft-response characteristics with those of automatic-control components is a necessity in many current applications, a comparison of the frequency-response curves of the aircraft as predicted by derivatives obtained from flight and wind-tunnel tests is of interest. Consideration is given herein to the ratio of pitching-velocity response to canard elevator deflection $\dot{\theta}/\delta$ as determined from equations involving two degrees of freedom longitudinally. This expression in terms of the differential operator $D = d/dt$ is (see ref. 10)

$$\frac{\dot{\theta}}{\delta} = \frac{K(\tau D + 1)}{D^2 + 2\zeta\omega_n D + \omega_n^2}$$

where

$$K = \frac{C_{m_\delta} C_{L_\alpha} - C_{m_\alpha} C_{L_\delta}}{\frac{I_y}{qS\bar{c}} \frac{mV}{qS}}$$

$$\tau = \frac{C_{m_\delta} \frac{mV}{qS} - C_{L_\delta} C_{m_{\dot{\alpha}}} \frac{\bar{c}}{2V}}{C_{m_\delta} C_{L_\alpha} - C_{m_\alpha} C_{L_\delta}}$$

[redacted]

$$2\zeta\omega_n = \frac{C_{L_\alpha}}{\frac{mV}{qS}} + \frac{-\left(C_{m_q} + C_{m_{\dot{\alpha}}}\right)\frac{\bar{c}}{2V}}{\frac{I_y}{qS\bar{c}}}$$

$$\omega_n^2 = \frac{-C_{L_\alpha}\, C_{m_q}\, \frac{\bar{c}}{2V}}{\frac{I_y}{qS\bar{c}}\ \frac{mV}{qS}} + \frac{-C_{m_\alpha}}{\frac{I_y}{qS\bar{c}}}$$

where ω_n and ζ correspond to the conventional undamped natural frequency and the damping ratio, respectively, and all stability derivatives are in radian measure.

Assuming C_{L_δ} to be zero, it is noted in the above expressions that τ becomes independent of C_{m_δ} leaving only the gain factor K being changed by the control effectiveness; therefore, the differences in C_{m_δ} as indicated from flight and tunnel tests produce only a scale change in the frequency-response function and do not affect the shapes of the frequency-response curves.

The calculations were made for a Mach number of 1.6 at sea level using the mass and inertia values given in reference 1, namely, $m = 5.05$ slugs and $I_y = 31.3$ slug-feet^2. Stability derivatives were defined for small and large angle-of-attack regions and may be read from figures 5 and 7. The damping-in-pitch derivatives were those presented in reference 1 for the two angle-of-attack regions. These frequency-response curves are presented as amplitude and phase against ω, the forcing frequency, in figure 12. It is noted that the K factor has not been included in these results.

These curves can illustrate effects of the nonlinearities noted in the stability derivatives, as well as the magnitude differences shown from flight and wind-tunnel data. The effects of the nonlinearities are compared by the curves for high and low angles of attack and illustrate that the location and magnitude of the resonant peaks are slightly different. The difference in resonant frequencies noted for the high-angle-of-attack comparisons is accounted for by the differences in values of C_{m_α}; the major portion of the peak-magnitude variations is caused by the damping factors. The maximum phase difference occurs near resonance. For many purposes of analysis these results are adequate.

[redacted]

CONCLUDING REMARKS

A comparison has been made between the supersonic longitudinal stability and control characteristics of a canard missile configuration as determined from free-flight tests of rocket-powered models and tests in a supersonic wind tunnel. The flight-test range included Mach numbers from 1.1 to about 1.6 representing a Reynolds number range from about 10×10^6 to 20×10^6, based on wing mean aerodynamic chord. The wind-tunnel tests were at Mach numbers of 1.62 and 1.93 with Reynolds numbers of 0.65×10^6 and 0.58×10^6, respectively.

Good correlation was shown between the two techniques for slopes of lift and moment coefficients against angle of attack and for aerodynamic-center location. The nonlinearities in these static stability derivatives due to angle of attack noted in the flight tests were also shown in the wind-tunnel tests and were present at the highest Mach number attained.

The control effectiveness of the deflected canard fins can be described as producing practically a pure moment or couple while of itself causing very little change in lift, the over-all lift effectiveness of the configuration being due to the ability of the canard fins to change the angle of attack. The average moment effectiveness of the canard fins as indicated by flight tests tended to be higher than shown by the wind-tunnel results.

The use of stability derivatives determined from flight and tunnel tests in predicting longitudinal frequency-response characteristics showed satisfactory agreement and would be adequate for many purposes of analysis.

Langley Aeronautical Laboratory
National Advisory Committee for Aeronautics
Langley Field, Va.

REFERENCES

1. Zarovsky, Jacob, and Gardiner, Robert A.: Flight Investigation of a Roll-Stabilized Missile Configuration at Varying Angles of Attack at Mach Numbers Between 0.8 and 1.79. NACA RM L50H21, 1951.

2. Niewald, Roy J., and Moul, Martin T.: The Longitudinal Stability, Control Effectiveness, and Control Hinge-Moment Characteristics Obtained From a Flight Investigation of a Canard Missile Configuration at Transonic and Supersonic Speeds. NACA RM L50I27, 1950.

3. Gardiner, Robert A., and Zarovsky, Jacob: Rocket-Powered Flight Test of a Roll-Stabilized Supersonic Missile Configuration. NACA RM L9K01a, 1950.

4. Rainey, Robert W.: Langley 9-Inch Supersonic Tunnel Tests of Several Modifications of a Supersonic Missile Having Tandem Cruciform Lifting Surfaces. Three-Component Data Results of Models Having Ratios of Wing Span to Tail Span Equal to and Less Than 1 and Some Static Rolling-Moment Data. NACA RM L50G07, 1951.

5. Nielsen, Jack N., Katzen, Elliott D., and Tang, Kenneth K.: Lift and Pitching-Moment Interference Between a Pointed Cylindrical Body and Triangular Wings of Various Aspect Ratios at Mach Numbers of 1.50 and 2.02. NACA RM A50F06, 1950.

6. Curfman, Howard J., Jr.: Theoretical and Analog Studies of the Effects of Nonlinear Stability Derivatives on the Longitudinal Motions of an Aircraft in Response to Step Control Deflections and to the Influence of Proportional Automatic Control. NACA RM L50L11, 1951.

7. Speth, Robert F.: Results of Rascal Supersonic Wind Tunnel Tests at M = 1.72. Rep. No. 56-980-001, Bell Aircraft Corp., Dec. 20, 1948.

8. Spahr, J. Richard, and Robinson, Robert A.: Wind-Tunnel Investigation at Mach Numbers of 1.5 and 2.0 of a Canard Missile Configuration. NACA RM A51C08, 1951.

9. Fischer, H. S.: Supersonic Wind-Tunnel Tests of a 0.075-Scale Model of the Nike 482 Missile. Rep. No. SM-13848, Douglas Aircraft Co. Inc., Nov. 27, 1950.

10. Seaberg, Ernest C., and Smith, Earl F.: Theoretical Investigation of an Automatic Control System With Primary Sensitivity to Normal Accelerations as Used To Control a Supersonic Canard Missile Configuration. NACA RM L51D23, 1951.

TABLE I.- COMPARISON OF FLIGHT AND WIND-TUNNEL MODELS

Characteristics	Model A (ref. 1)	Model B[a] (ref. 2)	Model C[a] (wind tunnel)
Diameter, in.	8	8	8
$\bar{c}$, ft	1.766	1.703	1.766
S, sq ft	4.110	3.780	4.110
S_f, sq ft	0.282	0.251	0.282
Span, in.	37.000	35.400	37.000
Length, in.	130.375	130.510	
Span/Diameter	4.625	4.430	4.625
c.g. location, $\bar{c}$ ahead of L.E. $\bar{c}$	0.384	0.622	0.568
Length from trailing edge of wing to trailing edge of canard fin, in. . . .	63.875	64.230	62.875

[a]Models B and C dimensions have been scaled to model A by the ratio of diameters.

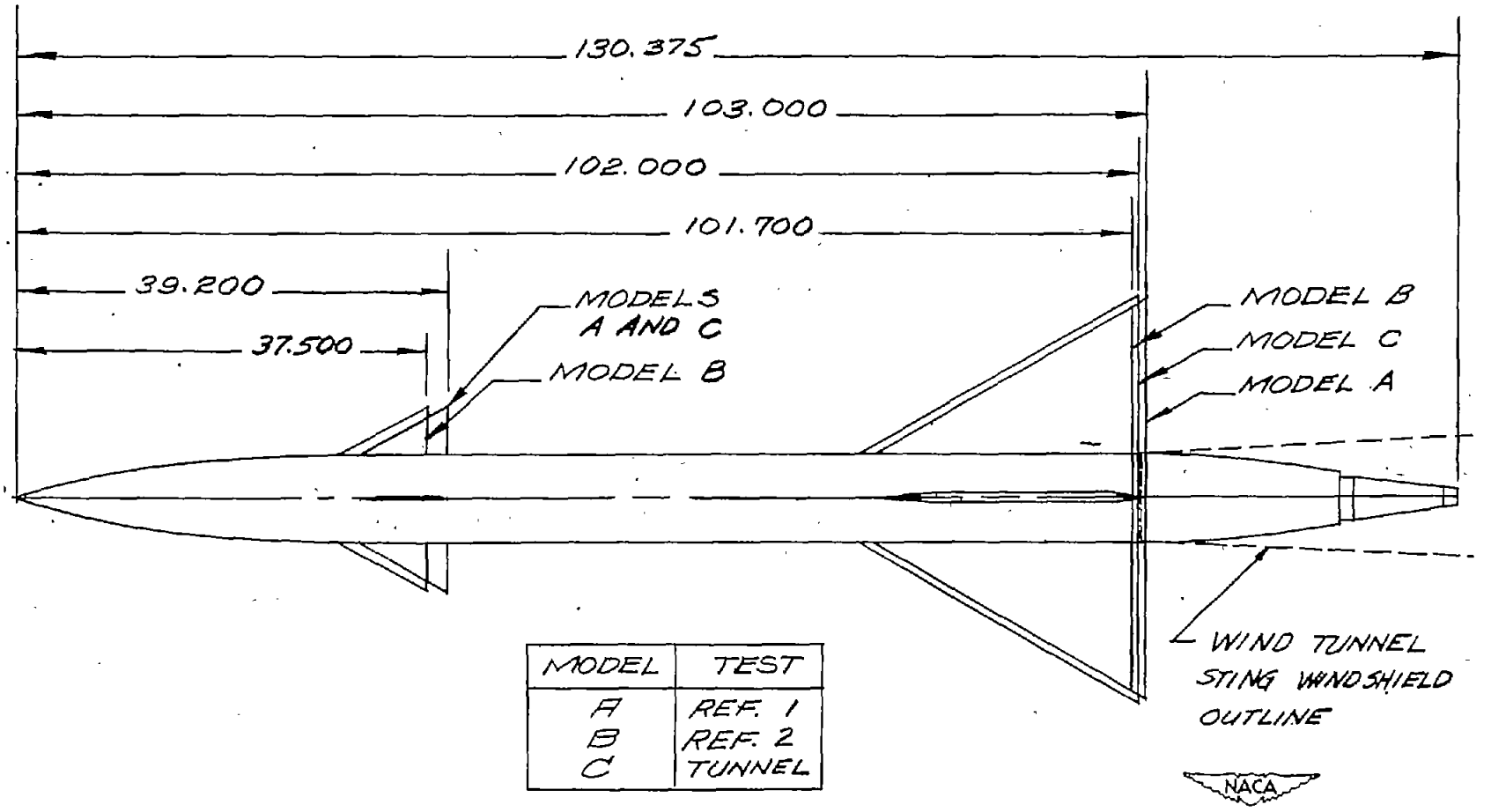

Figure 1.- Comparison of geometry of flight models (refs. 1 and 2) and wind-tunnel model. Models B and C are drawn scaled to the diameter of model A. All dimensions are in inches.

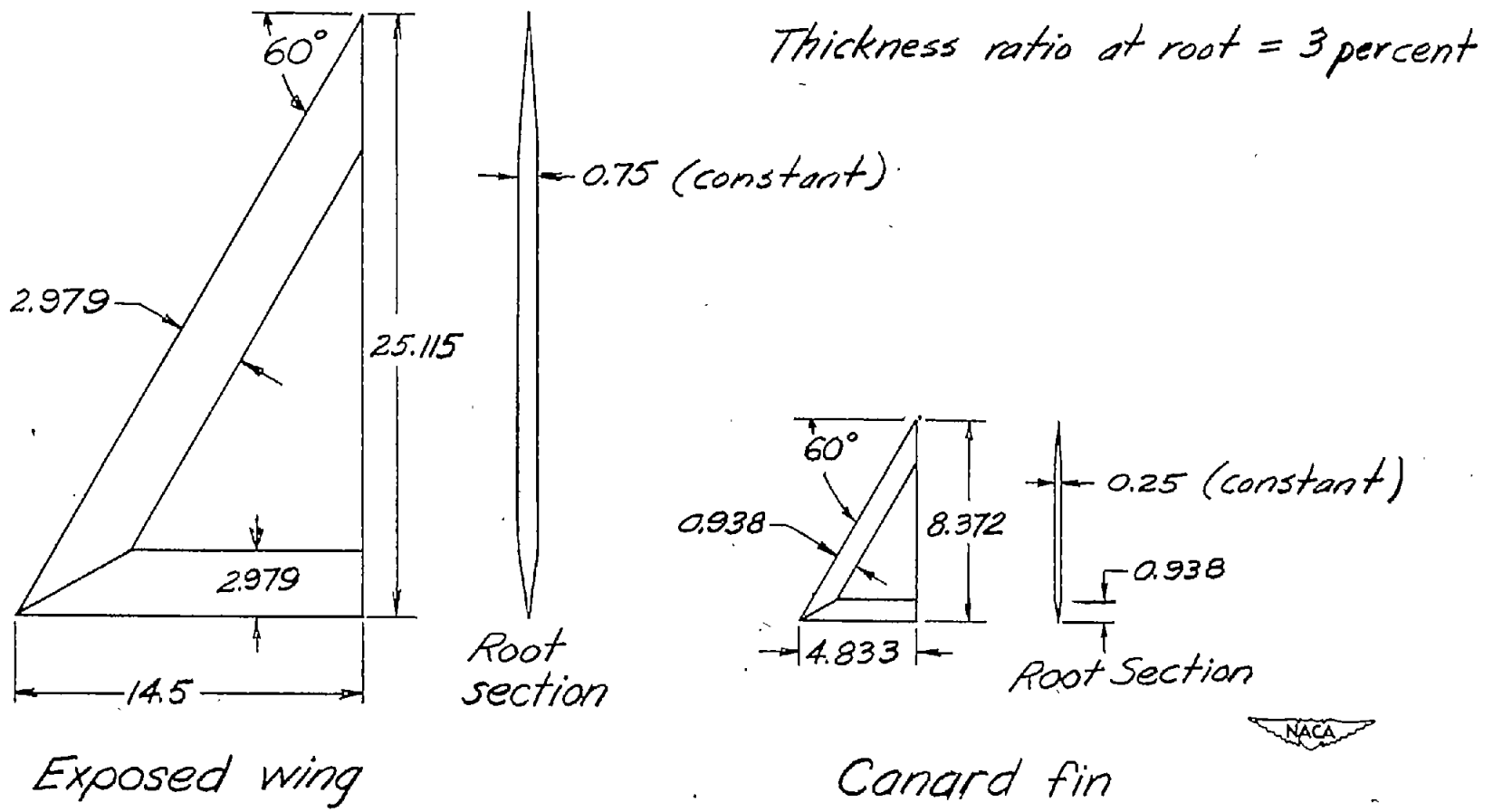

Figure 2.- Sketch of wing and canard fins. All dimensions are in inches and correspond to those of model A.

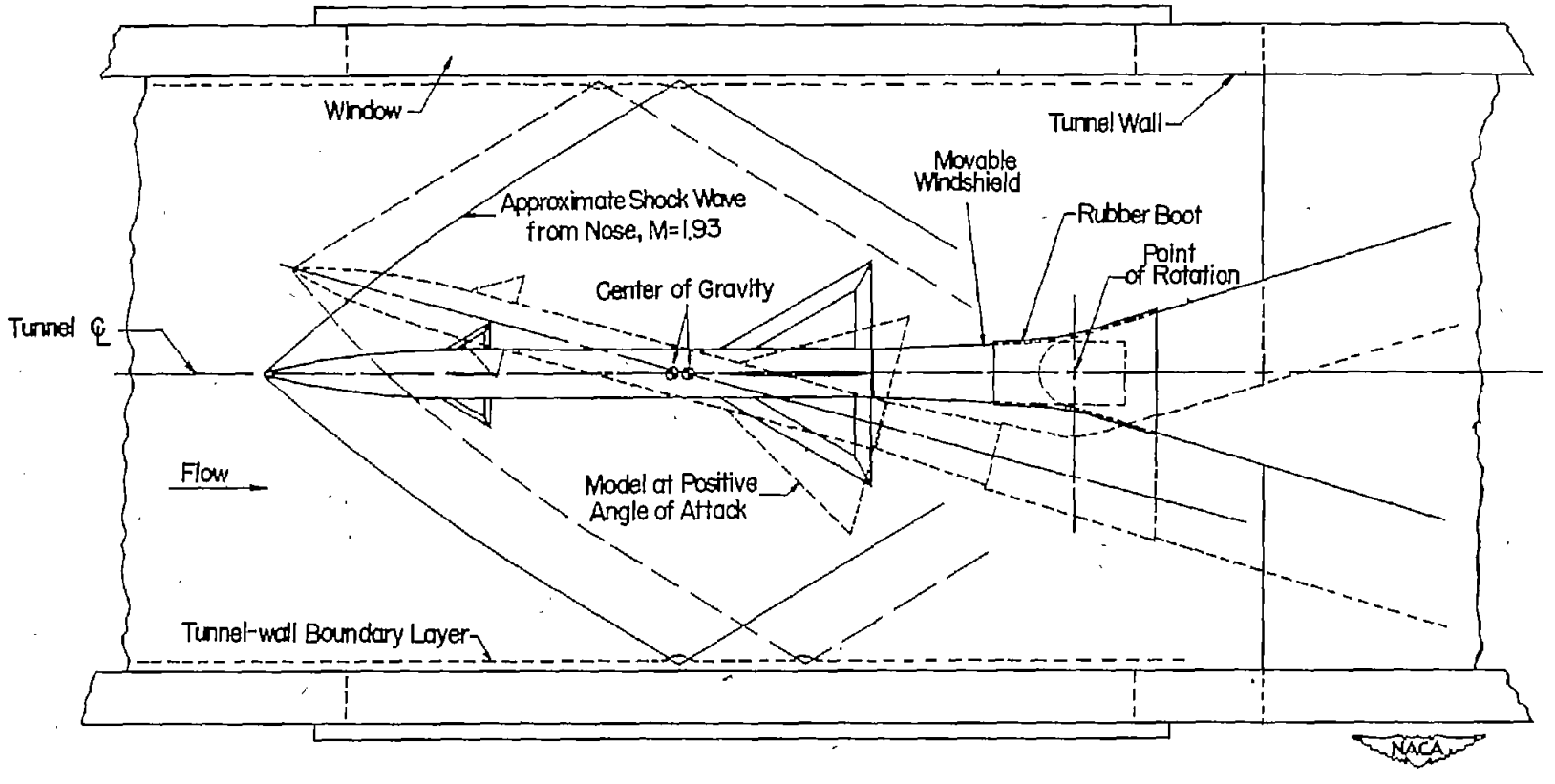

Figure 3.- Model installation in tunnel.

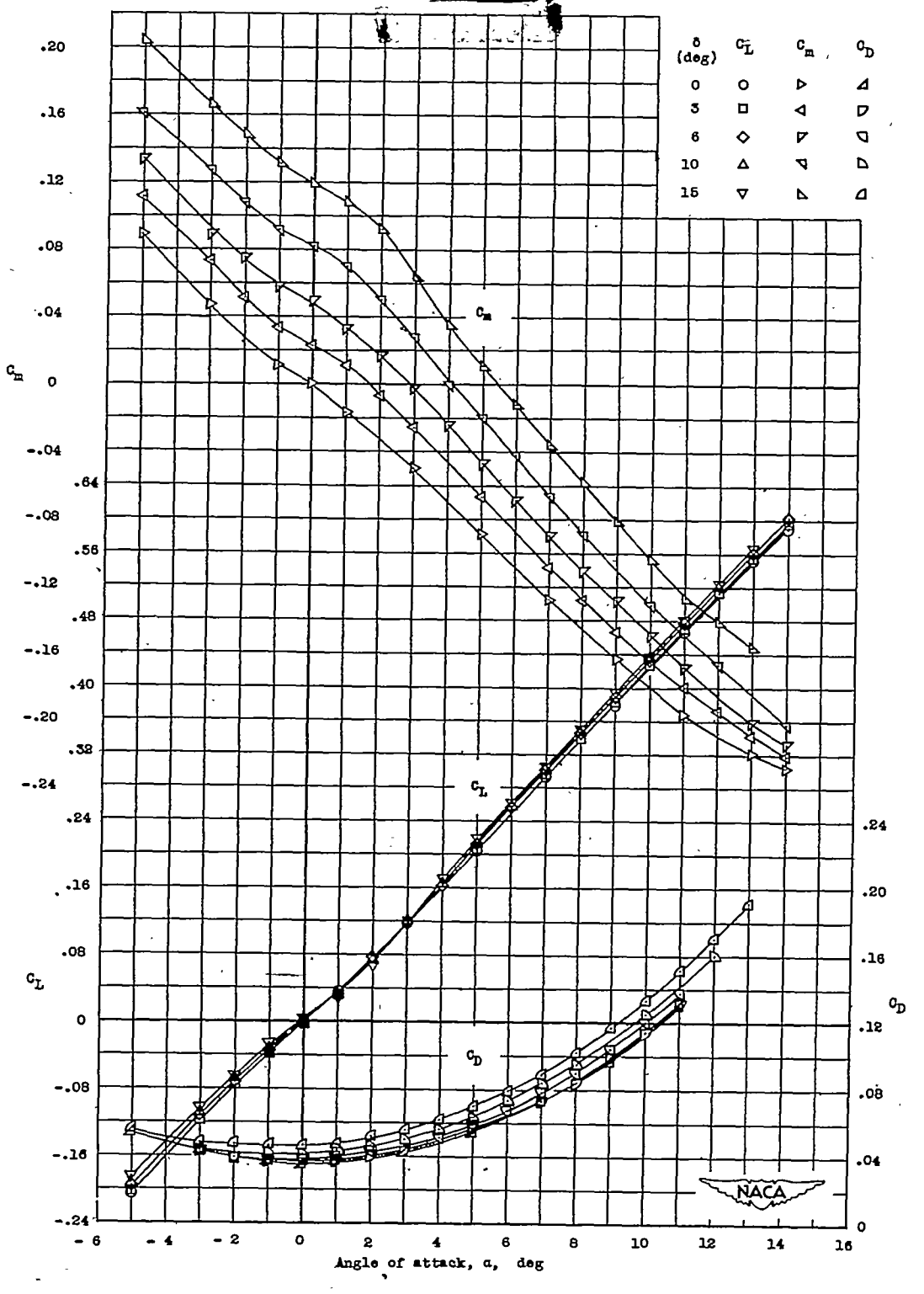

(a) M = 1.62.

Figure 4.- Wind-tunnel results. Pitching moments are about a center of gravity located 0.568$\bar{c}$ ahead of the leading edge of $\bar{c}$.

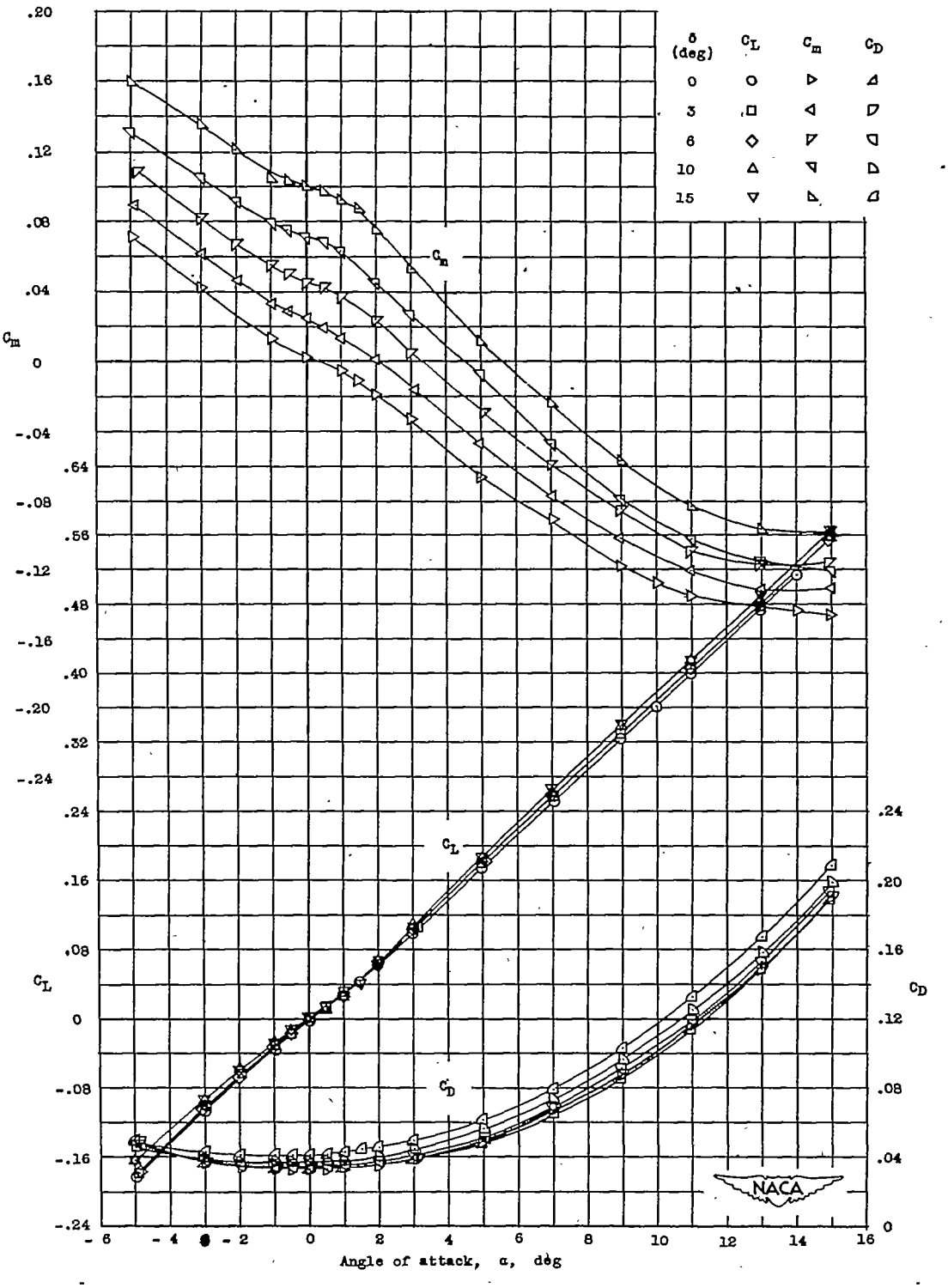

(b) M = 1.93.

Figure 4.- Concluded.

[redacted]

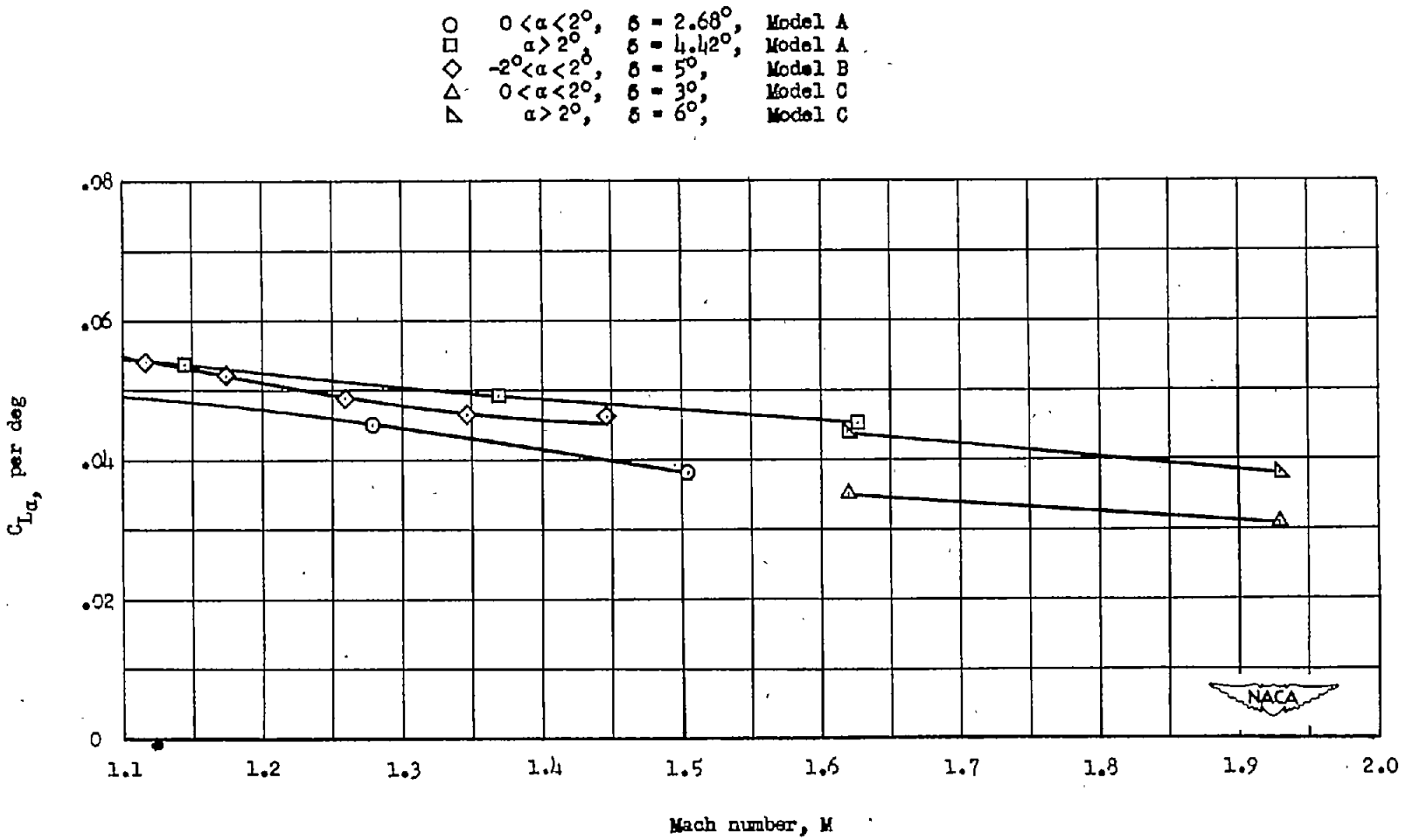

Figure 5.- Variation of lift-curve slope with Mach number.

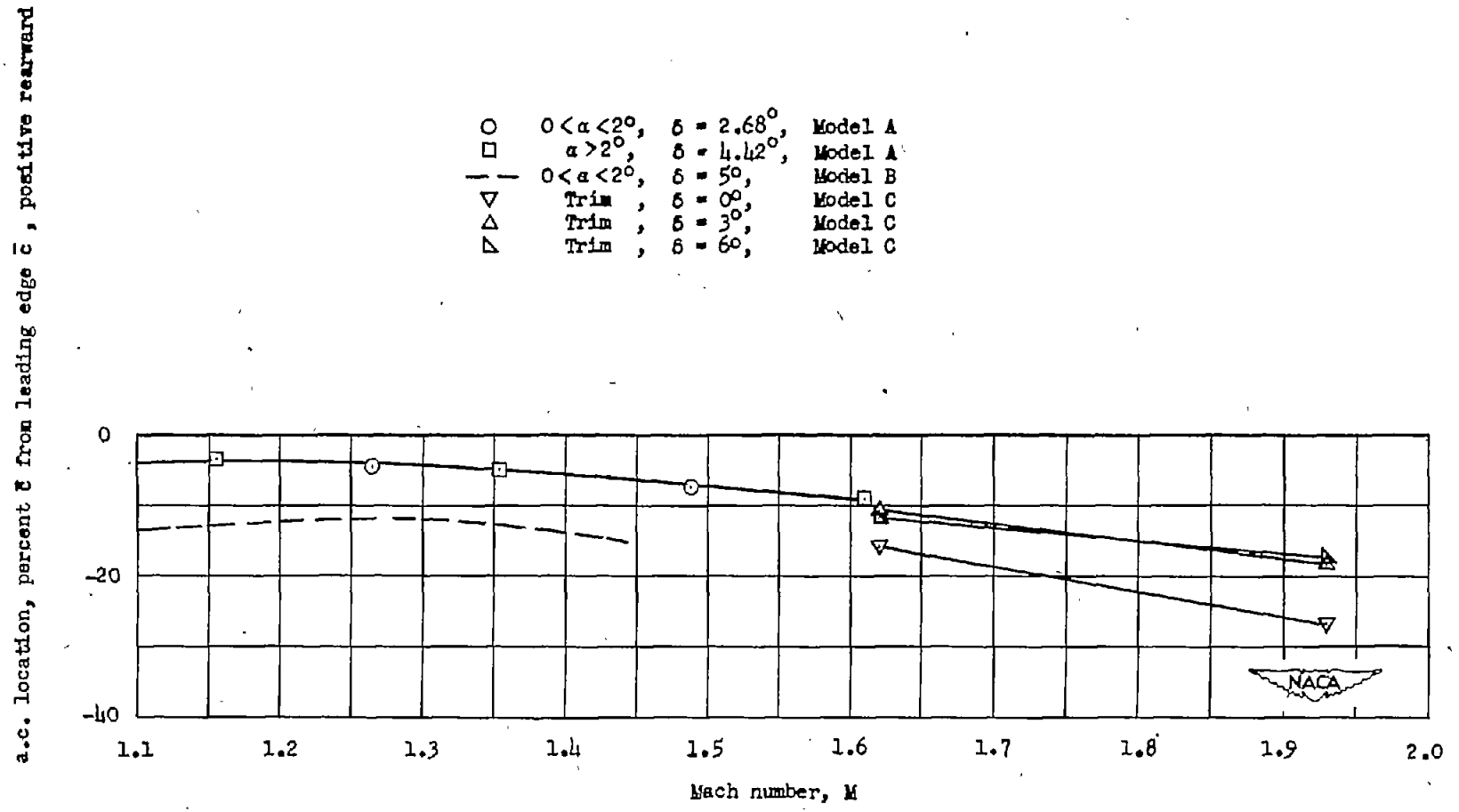

Figure 6.- Variation of aerodynamic-center location with Mach number.

CONFIDENTIAL

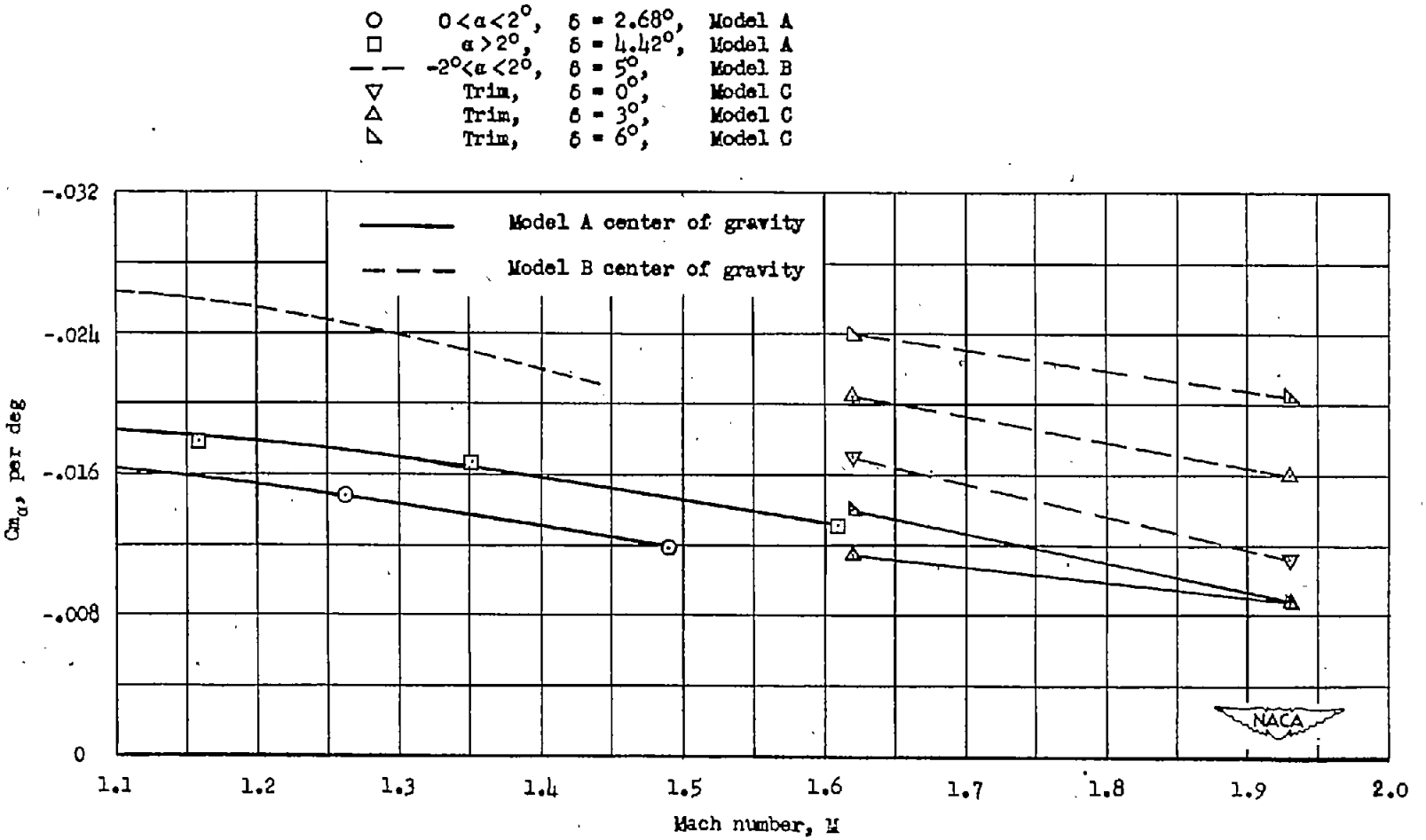

Figure 7.- Variation of static-stability parameter with Mach number.

CONFIDENTIAL

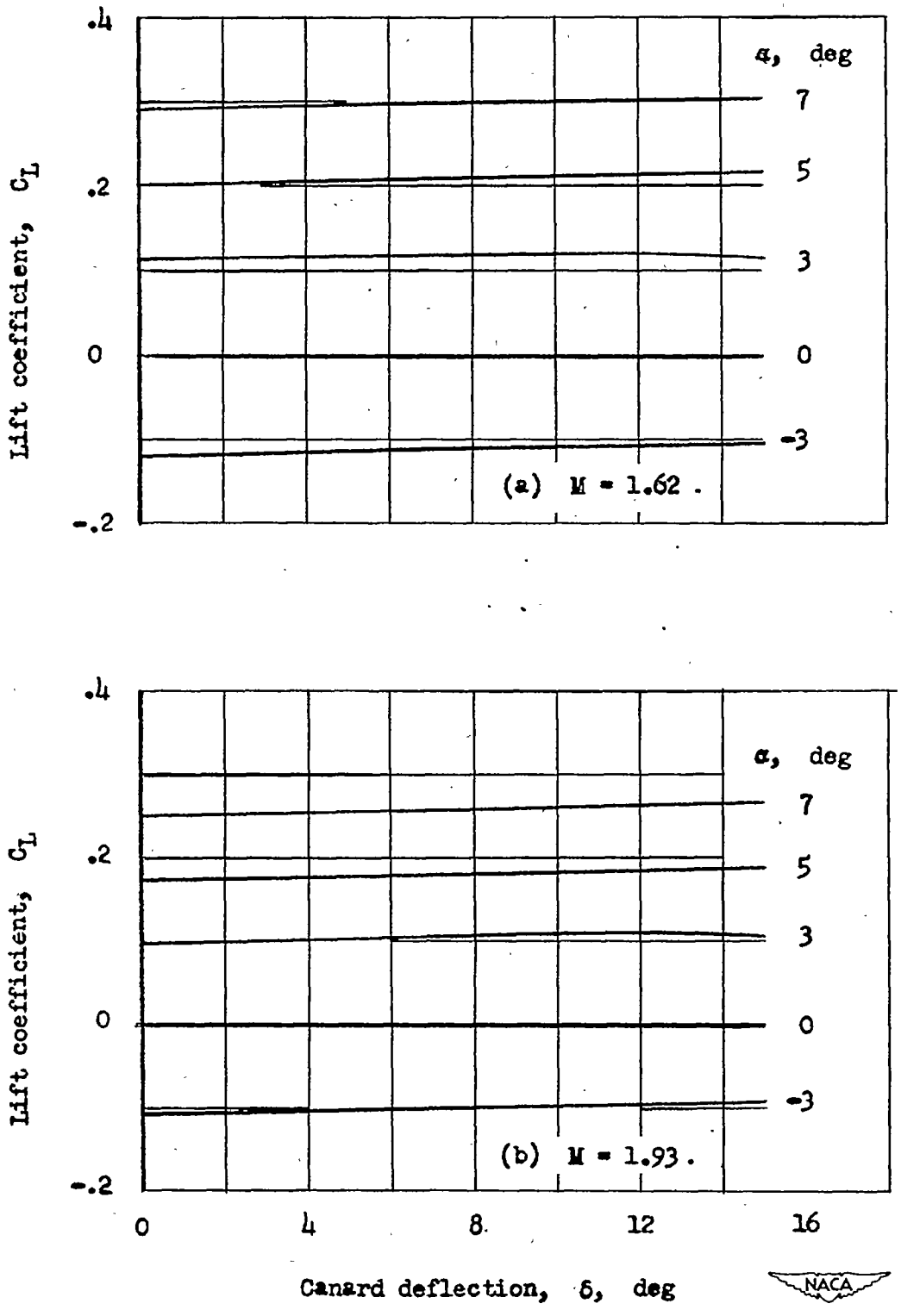

Figure 8.- Variation of lift coefficient with canard fin deflection at constant angles of attack from wind-tunnel tests.

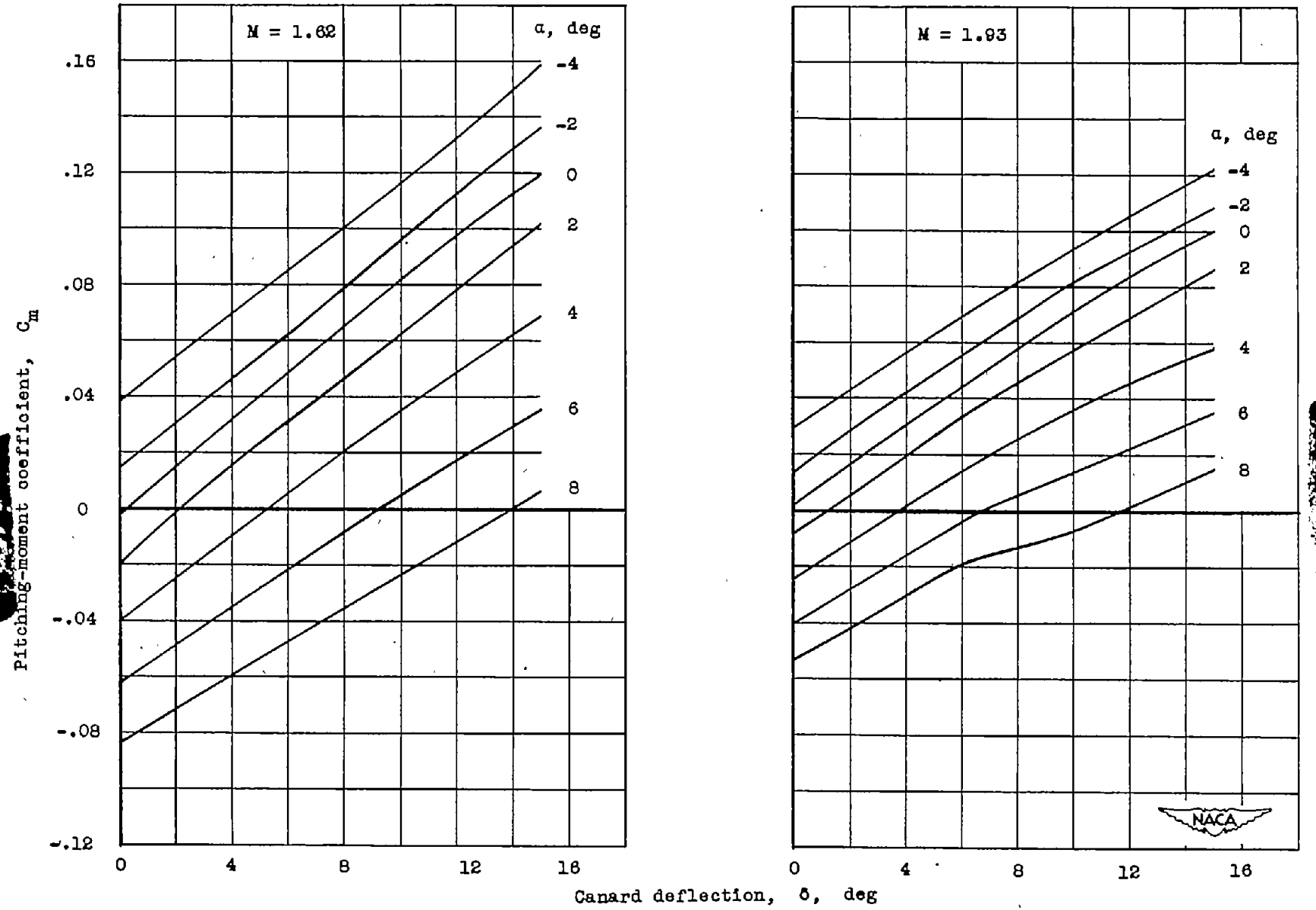

(a) Model A center of gravity.

Figure 9.- Variation of pitching-moment coefficient with canard fin deflection for constant angles of attack from wind-tunnel tests.

[redacted]

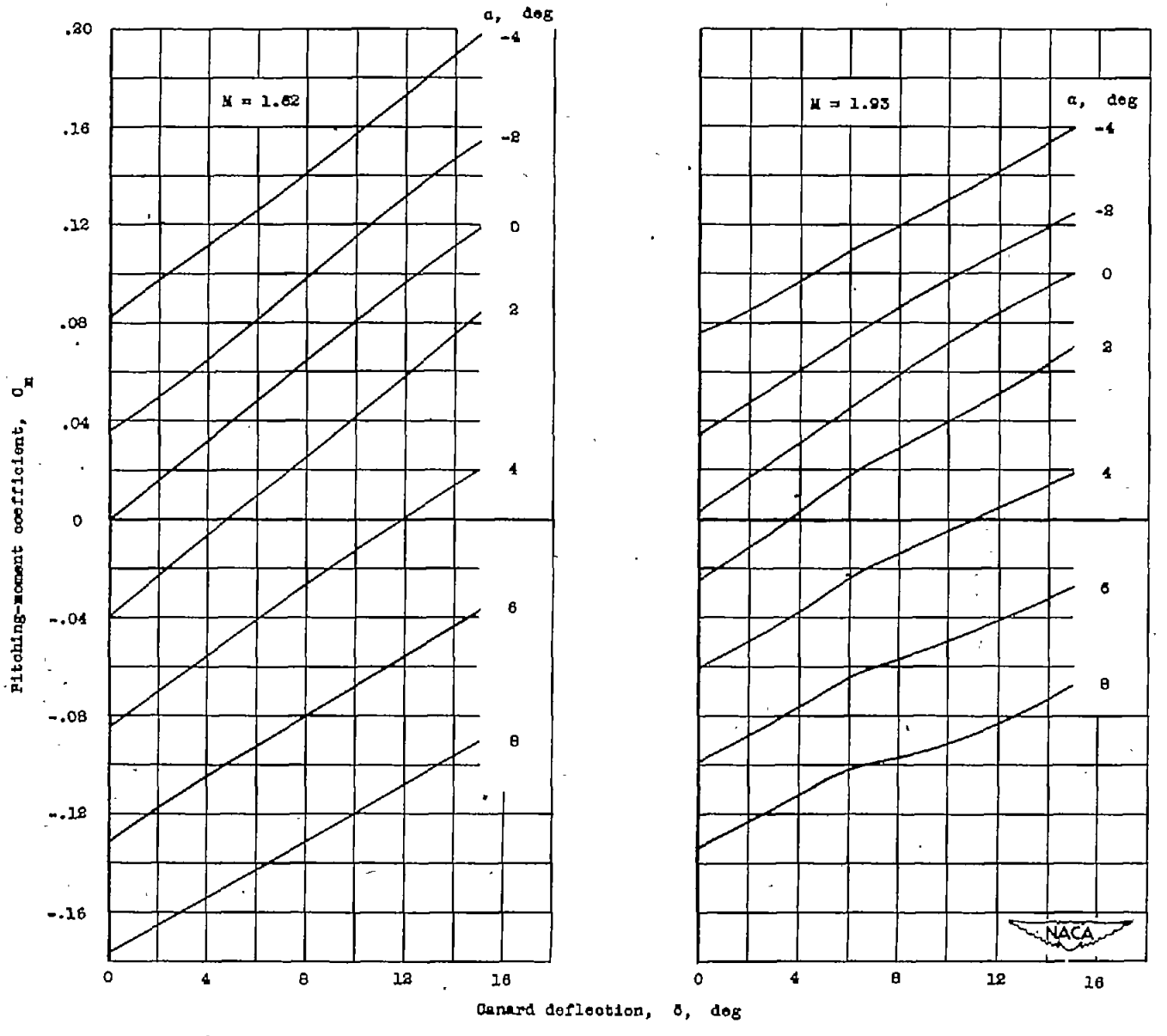

(b) Model B center of gravity.

Figure 9.- Concluded.

[redacted]

CONFIDENTIAL

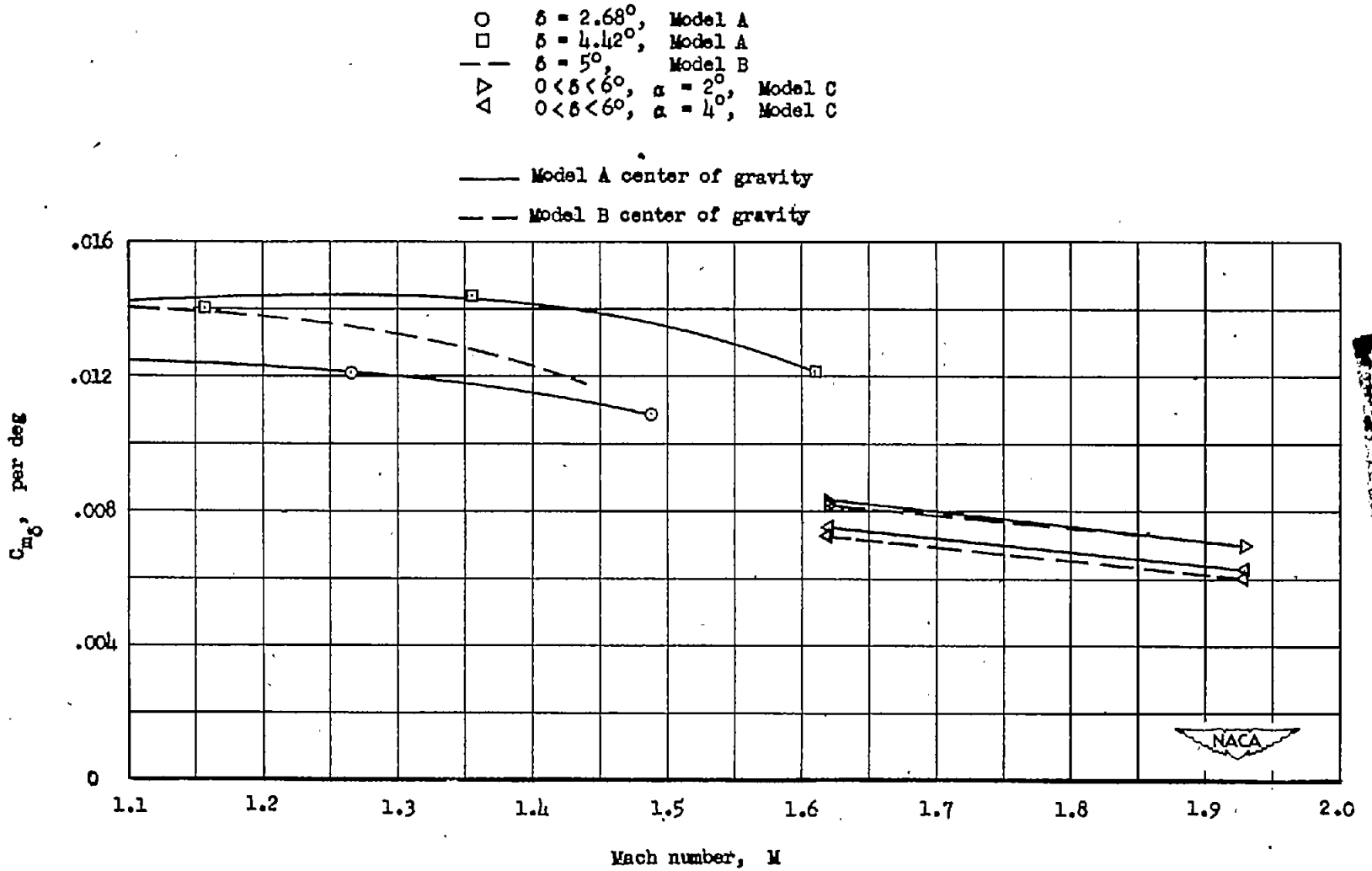

Figure 10.- Variation of control-effectiveness parameter with Mach number.

CONFIDENTIAL

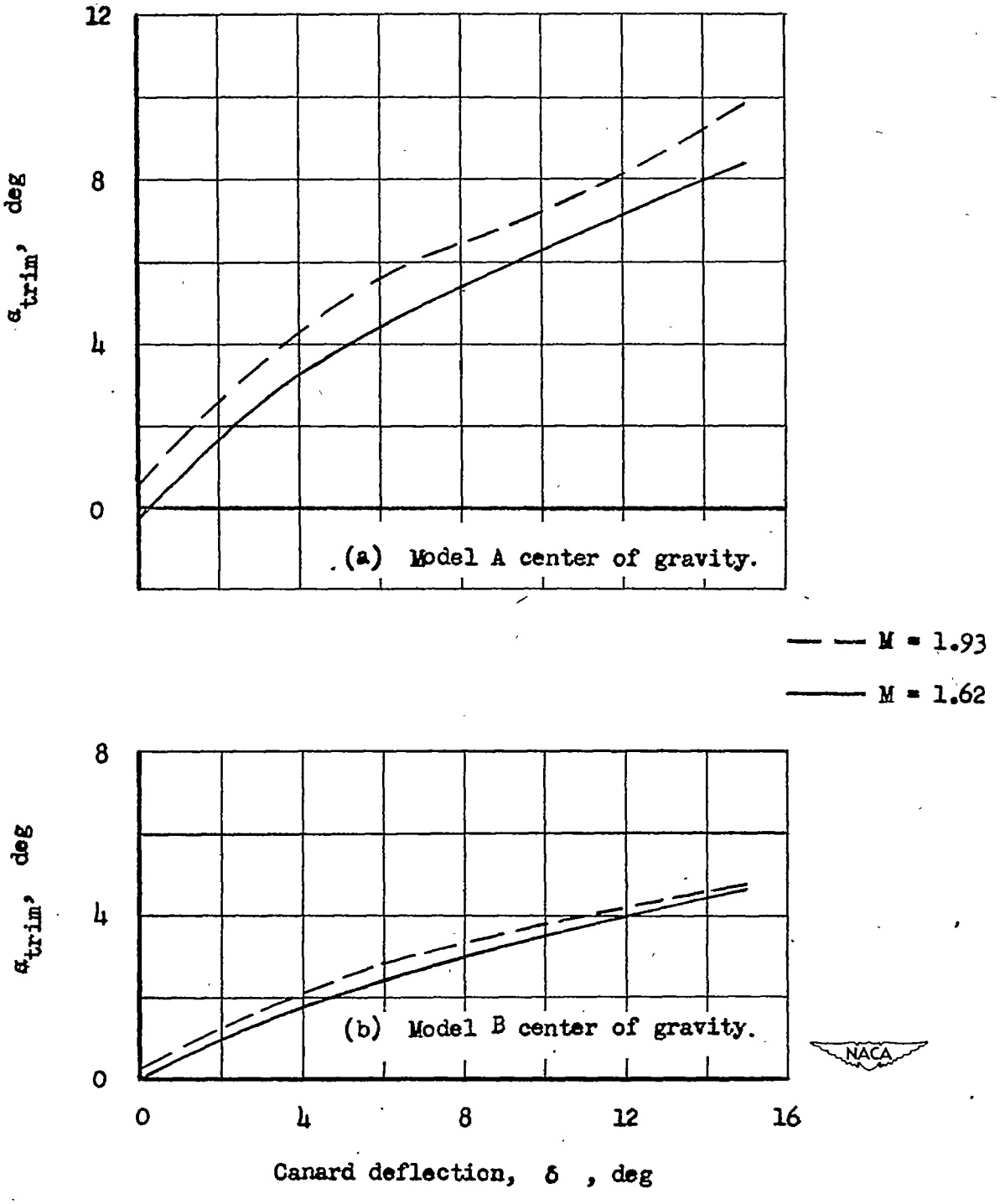

Figure 11.- Variation of trim angle of attack with canard fin deflection from wind-tunnel tests.

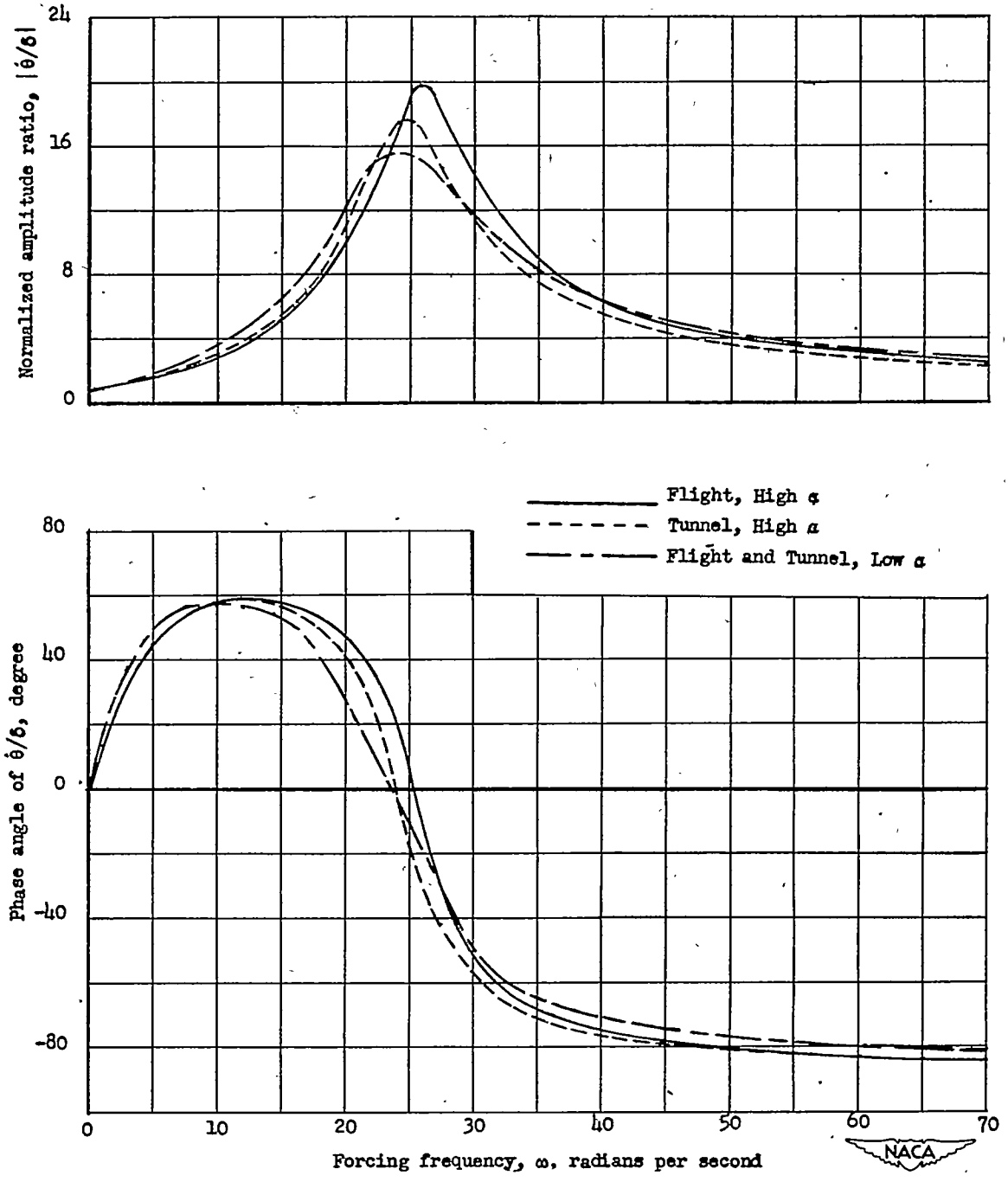

Figure 12.- Comparison of flight and wind-tunnel results in predicting the pitching velocity per unit canard-fin-deflection frequency response.

NACA-Langley - 8-8-52 - 300